Smart Mater. Struct. 14 (2005) 1410–1420 doi:10.1088/0964-1726/14/6/034

Static shape control of repetitive structures integrated with piezoelectric actuators

Dingkao Jin[1], Dongchang Sun[2,3], Weimin Chen[1], Dajun Wang[1] and Liyong Tong[2]

[1] State Key Laboratory for Turbulence and Complex Systems/Department of Mechanics and Engineering Science, Peking University, Beijing 100871, People's Republic of China
[2] School of Aerospace, Mechanical and Mechatronic Engineering, The University of Sydney, NSW 2006, Australia

E-mail: Dsun@aeromech.usyd.edu.au

Received 24 November 2003, in final form 23 August 2005
Published 9 November 2005
Online at stacks.iop.org/SMS/14/1410

Abstract
In this paper, several simplification methods are presented for shape control of repetitive structures such as symmetrical, rotational periodic, linear periodic, chain and axisymmetrical structures. Some special features in the differential equations governing these repetitive structures are examined by considering the whole structures. Based on the special properties of the governing equations, several methods are presented for simplifying their solution process. Finally, the static shape control of a cantilever symmetrical plate with piezoelectric actuator patches is demonstrated using the present simplification method. The result shows that present methods can effectively be used to find the optimal control voltage for shape control.

1. Introduction

Research on shape control of flexible structures has received much attention particularly in aircraft and space engineering [1–4]. Shape control of a structure is to apply control forces to make its shape trace an objective shape or to keep a designated shape under external disturbances. In recent years, piezoelectric materials have been widely used in shape control of structures due to their light weight and quick response to actuating voltage. Several methods have been developed and applied to find the optimal control voltages for shape control of smart structures integrated with piezoelectric actuators [5–11].

Repetitive structures are often encountered in engineering environments which are composed of a set of components with identical geometric shape, physical property, boundary conditions and even interactions with each other. Since many space structures or structural components such as space antennae, solar array and many parts in rockets and satellites fall in repetitive structures, investigation of shape control of repetitive structures is very important.

In general, shape control of a structure must be designed and performed based on modeling of the entire structure. However, shape control of a repetitive structure can be designed by considering only one of its substructures due to its repetitive feature, and hence numerical and experimental costs can be significantly reduced. A large amount of literature can be found on the solution of the natural frequencies and modal shapes of repetitive structures. Evenson [12] studied the vibration problems of symmetrical structures, Thomas [13] investigated vibration of revolutionary periodic structures, and Cai and his colleagues [14–16] also carried out research into the vibration of revolutionary periodic structures using the U-transformation. Recently, Wang and Wang [17] presented a reduction method for natural vibration of symmetrical and linking structures.

Since shape control of repetitive structures is a new topic, there is no literature about this topic available so far. This paper aims to simplify the shape control of repetitive structures including mirror-reflected symmetrical (symmetrical for short hereafter), rotational periodic, linear periodic and linking as well as axisymmetrical structures by fully utilizing their symmetrical characteristics. Shape control of repetitive structures is investigated systematically and theoretically,

[3] Author to whom any correspondence should be addressed.

and some methods are presented to simplify the numerical computation and on-line shape control. It is demonstrated that the shape control problem of repetitive structures can be reduced to shape control of one of its substructures when the actuator placement and inputted control forces also have the same repetitive feature as the structure. The present methods can remarkably reduce the dimensions of the control system in shape control of repetitive structures, and consequently simplify the related theoretical and experimental analysis.

2. Symmetrical structures

2.1. Modeling and governing equations

A symmetrical structure can be defined as a structure whose geometric shape, physical properties and boundary conditions are symmetrical about a plane or line, referred to as the symmetrical plane or line. Moreover, assume that the actuators are also symmetrically collocated. An example of a symmetrical piezoelectrically actuated structure is illustrated in figure 1. In this case, the entire structure can be treated as two substructures, and two Cartesian coordinate systems are set, respectively, in substructure 1 and 2. The directions of their y and z axes in these two coordinate systems are the same, while those of their x axes are opposite to each other. Their equilibrium equations together with corresponding boundary conditions, which bridge the displacements and the control forces, can be expressed in the following form:

$$\boldsymbol{L}\boldsymbol{w}_i + \boldsymbol{B}\boldsymbol{U}_i = 0 \qquad \text{in } \Omega, \qquad i = 1, 2 \tag{1}$$

$$\boldsymbol{\Gamma}\boldsymbol{w}_i = 0 \qquad \text{on } \partial\Omega, \qquad i = 1, 2 \tag{2}$$

where $\boldsymbol{w}_1 \in R^n$ and $\boldsymbol{w}_2 \in R^n$ are functions or function vectors consisting of the generalized displacements of these two substructures, Ω is the domain of a substructure, $\partial\Omega$ represents its boundary excluding the common boundary where x is equal to zero, $\boldsymbol{L}$, $\boldsymbol{B}$ and $\boldsymbol{\Gamma}$ represent the elasticity, control and boundary differential operator matrices, respectively, and $\boldsymbol{U}_i \in R^m$ is the function vector of actuating forces induced by the actuators. For discrete models, the function vectors $\boldsymbol{w}_i$ and $\boldsymbol{U}_i$ as well as the differential operator matrices $\boldsymbol{L}$, $\boldsymbol{B}$ and $\boldsymbol{\Gamma}$ in equations (1) and (2) become ordinary numerical vectors and matrices, respectively.

In addition, the generalized displacements and actuating forces of these two substructures at their common boundary (say $x = 0$) should satisfy the continuity conditions given by

$$\boldsymbol{J}_1\boldsymbol{w}_1 = -\boldsymbol{J}_1\boldsymbol{w}_2 \qquad \text{on } x = 0 \tag{3}$$

$$\boldsymbol{J}_2\boldsymbol{w}_1 = \boldsymbol{J}_2\boldsymbol{w}_2 \qquad \text{on } x = 0 \tag{4}$$

where $\boldsymbol{J}_1$ and $\boldsymbol{J}_2$ are the boundary operator matrices. If there are $2l$ elastic and rigid linkages between these two substructures at points s_j $(j = 1, 2, \ldots l)$, the following constraining conditions should be imposed:

$$\boldsymbol{J}_{rj}\boldsymbol{w}_1|_{s_j} = \overline{\boldsymbol{J}}_{rj}\boldsymbol{w}_2|_{\overline{s}_j}, \qquad j = 1, 2 \ldots l \tag{5}$$

$$\overline{\boldsymbol{J}}_{rj}\boldsymbol{w}_1|_{\overline{s}_j} = \boldsymbol{J}_{rj}\boldsymbol{w}_2|_{s_j}, \qquad j = 1, 2 \ldots l. \tag{6}$$

Due to the existence of continuity and constraining conditions, $\boldsymbol{w}_1$ and $\boldsymbol{w}_2$ are coupled to each other. Equations (1)–(6) give all the governing equations for a symmetrical structure.

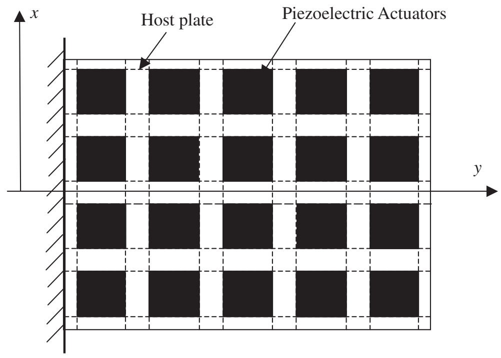

Figure 1. A symmetrical structure.

2.2. Simplification of the shape control problem

Using the symmetry of the structures, their shape control problem can be simplified. To this end, take the following transformation in the generalized displacements of the original structure:

$$\boldsymbol{w} = \begin{Bmatrix} \boldsymbol{w}_1 \\ \boldsymbol{w}_2 \end{Bmatrix} = \boldsymbol{S}_{2n}\boldsymbol{q} \tag{7}$$

where $\boldsymbol{S}_{2n}$ is a transformation matrix given by

$$S_{2n} = \frac{1}{\sqrt{2}}\begin{bmatrix} \boldsymbol{I}_n & \boldsymbol{I}_n \\ \boldsymbol{I}_n & -\boldsymbol{I}_n \end{bmatrix} \tag{8}$$

and $\boldsymbol{I}_n$ is the identity matrix whose dimension is the same as that of the displacement function vector. The displacements can be expressed in terms of a symmetrical generalized displacement $\boldsymbol{q}_1$ and anti-symmetrical one $\boldsymbol{q}_2$, respectively, i.e.,

$$w = \frac{1}{\sqrt{2}}\begin{bmatrix} \boldsymbol{I}_n \\ \boldsymbol{I}_n \end{bmatrix}\boldsymbol{q}_1 + \frac{1}{\sqrt{2}}\begin{bmatrix} \boldsymbol{I}_n \\ -\boldsymbol{I}_n \end{bmatrix}\boldsymbol{q}_2. \tag{9}$$

Similarly, taking the same transformation in the input $\boldsymbol{U}$ gives

$$\boldsymbol{U} = \begin{Bmatrix} \boldsymbol{U}_1 \\ \boldsymbol{U}_2 \end{Bmatrix} = \boldsymbol{S}_{2m}\boldsymbol{V} = \frac{1}{\sqrt{2}}\begin{bmatrix} \boldsymbol{I}_m & \boldsymbol{I}_m \\ \boldsymbol{I}_m & -\boldsymbol{I}_m \end{bmatrix}\begin{Bmatrix} \boldsymbol{v}_1 \\ \boldsymbol{v}_2 \end{Bmatrix}$$
$$= \frac{1}{\sqrt{2}}\begin{bmatrix} \boldsymbol{I}_m \\ \boldsymbol{I}_m \end{bmatrix}\boldsymbol{v}_1 + \frac{1}{\sqrt{2}}\begin{bmatrix} \boldsymbol{I}_m \\ -\boldsymbol{I}_m \end{bmatrix}\boldsymbol{v}_2 \tag{10}$$

where $\boldsymbol{I}_m$ is a identity matrix with dimension m. It is noted that the transformation matrix $\boldsymbol{S}_{2n}$ is an orthogonal matrix, i.e. it satisfies

$$S_{2n}^{\mathrm{T}}\boldsymbol{S}_{2n} = \boldsymbol{I}_{2n}; \qquad S_{2m}^{\mathrm{T}}\boldsymbol{S}_{2m} = \boldsymbol{I}_{2m}. \tag{11}$$

Equations (1)–(4) can be rewritten into the following forms:

$$\begin{bmatrix} \boldsymbol{L} & \boldsymbol{0} \\ \boldsymbol{0} & \boldsymbol{L} \end{bmatrix}\begin{Bmatrix} \boldsymbol{w}_1 \\ \boldsymbol{w}_2 \end{Bmatrix} + \begin{bmatrix} \boldsymbol{B} & \boldsymbol{0} \\ \boldsymbol{0} & \boldsymbol{B} \end{bmatrix}\begin{Bmatrix} \boldsymbol{U}_1 \\ \boldsymbol{U}_2 \end{Bmatrix} = \boldsymbol{0} \qquad \text{in } \Omega \tag{12a}$$

$$\begin{bmatrix} \Gamma & \boldsymbol{0} \\ \boldsymbol{0} & \Gamma \end{bmatrix}\begin{Bmatrix} \boldsymbol{w}_1 \\ \boldsymbol{w}_2 \end{Bmatrix} = \boldsymbol{0} \qquad \text{on } \partial\Omega \tag{12b}$$

$$\begin{bmatrix} \boldsymbol{J}_1 & \boldsymbol{J}_1 \\ \boldsymbol{J}_2 & -\boldsymbol{J}_2 \end{bmatrix}\begin{Bmatrix} \boldsymbol{w}_1 \\ \boldsymbol{w}_2 \end{Bmatrix} = \boldsymbol{0} \qquad \text{on } x = 0 \tag{12c}$$

$$\begin{bmatrix} \boldsymbol{J}_{rj} & \boldsymbol{0} \\ \boldsymbol{0} & \boldsymbol{J}_{rj} \end{bmatrix}\begin{Bmatrix} \boldsymbol{w}_1 \\ \boldsymbol{w}_2 \end{Bmatrix}\Bigg|_{s_j} = \begin{bmatrix} \overline{\boldsymbol{J}}_{rj} & \boldsymbol{0} \\ \boldsymbol{0} & \overline{\boldsymbol{J}}_{rj} \end{bmatrix}\begin{bmatrix} \boldsymbol{0} & \boldsymbol{I}_n \\ \boldsymbol{I}_n & \boldsymbol{0} \end{bmatrix}\begin{Bmatrix} \boldsymbol{w}_1 \\ \boldsymbol{w}_2 \end{Bmatrix}\Bigg|_{\overline{s}_j},$$
$$j = 1, 2, \ldots l. \tag{12d}$$

Substituting equations (7) and (10) into (12), and noting (11), we have

$$
\begin{aligned}
&\boldsymbol{L}\boldsymbol{q}_i + \boldsymbol{B}\boldsymbol{v}_i = \boldsymbol{0} \qquad \text{in } \Omega\\
&\boldsymbol{\Gamma}\boldsymbol{q}_i = \boldsymbol{0} \qquad \text{on } \partial\Omega; \quad i = 1, 2\\
&\boldsymbol{J}_i\boldsymbol{q}_i = \boldsymbol{0} \qquad \text{on } x = 0\\
&\boldsymbol{J}_{rj}\boldsymbol{q}_i|_{s_j} = \pm\overline{\boldsymbol{J}}_{rj}\boldsymbol{q}_i|_{\bar{s}_j}, \qquad + \text{ for } i = 1, \quad - \text{ for } i = 2;\\
&j = 1, 2, \ldots, l.
\end{aligned} \tag{13}
$$

Equation (13) gives two sets of decoupled equations in terms of $\boldsymbol{q}_1$ and $\boldsymbol{q}_2$, respectively, which shows that the shape control problem of an entire symmetrical structure depicted in equations (12) can be converted to the shape control problem of its two substructures given in equation (13). $i = 1$ gives the symmetrical displacements, and $i = 2$ the anti-symmetrical displacements. The feature given above can be used to significantly simplify the shape control of symmetrical structures.

In the static shape control of such a symmetrical structure, the target shape can be expressed by the symmetrical desired displacement vector as follows:

$$
w_d = (w_{d1}, w_{d2})^{\mathrm{T}}. \tag{14}
$$

The desired generalized displacements can be obtained from the inverse of equation (9),

$$
\boldsymbol{q}_d = \begin{Bmatrix} \boldsymbol{q}_{d1} \\ \boldsymbol{q}_{d2} \end{Bmatrix} = \boldsymbol{S}_{2n}^{T}\boldsymbol{w}_d = \frac{1}{\sqrt{2}}\begin{bmatrix} \boldsymbol{I}_n \\ \boldsymbol{I}_n \end{bmatrix}\boldsymbol{w}_{d1} + \frac{1}{\sqrt{2}}\begin{bmatrix} \boldsymbol{I}_n \\ -\boldsymbol{I}_n \end{bmatrix}\boldsymbol{w}_{d2}. \tag{15}
$$

The shape control problem of a whole symmetrical structure in equations (12) is simplified to two shape control problems of its substructures described by equations (13) with desired displacements $\boldsymbol{q}_{di}$ given in equation (15).

As a special case, take a symmetric structure discretized by the finite element method as an example to illustrate the design process of the actuating forces for its static shape control. In this case, the operator matrices $\boldsymbol{L}$, $\boldsymbol{B}$, $\boldsymbol{\Gamma}$ and $\boldsymbol{J}$ in equation (13) are numerical matrices.

After taking the corresponding transformations, the boundary conditions, continuity conditions and constraining equations can be assembled into the equilibrium equations described by

$$
\boldsymbol{L}_{gi}\boldsymbol{q}_i + \boldsymbol{B}\boldsymbol{v}_i = 0 \qquad i = 1, 2 \tag{16}
$$

where $\boldsymbol{q}_i$ is the generalized displacement vector and $\boldsymbol{L}_{gi}$ is the global stiffness matrix. If the structure is properly constrained so that the stiffness matrix is nonsingular, the generalized displacements can be solved from equation (16) as

$$
\boldsymbol{q}_i = -\boldsymbol{L}_{gi}^{-1}\boldsymbol{B}\boldsymbol{v}_i. \tag{17}
$$

To measure the difference between the actuated shape and the desired one, an error function is defined as follows.

$$
e_i = (\boldsymbol{q}_i - \boldsymbol{q}_{di})^{\mathrm{T}}(\boldsymbol{q}_i - \boldsymbol{q}_{di}), \qquad i = 1, 2. \tag{18}
$$

Substituting equation (17) into (18) and letting the derivative of the error function with respect to $\boldsymbol{v}_i$ be zero, the optimal actuating forces can be easily obtained in the following form:

$$
\boldsymbol{v}_i = -\left[\boldsymbol{B}^{\mathrm{T}}\boldsymbol{L}_{gi}^{-T}\boldsymbol{L}_{gi}^{-1}\boldsymbol{B}\right]^{-1}\boldsymbol{B}^{\mathrm{T}}\boldsymbol{L}_{gi}^{-T}\boldsymbol{q}_{di}, \qquad i = 1, 2. \tag{19}
$$

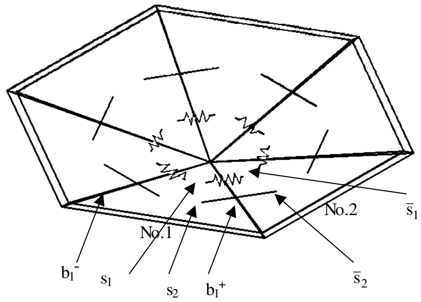

Figure 2. A rotational periodic structure.

Substituting equation (19) into (10) yields

$$
\begin{aligned}
\boldsymbol{U} &= \boldsymbol{S}_{2m}\begin{Bmatrix} \boldsymbol{v}_1 \\ \boldsymbol{v}_2 \end{Bmatrix}\\
&= -\frac{1}{\sqrt{2}}\begin{bmatrix} \boldsymbol{I}_m \\ \boldsymbol{I}_m \end{bmatrix}\left[\boldsymbol{B}^{\mathrm{T}}\boldsymbol{L}_{g1}^{-T}\boldsymbol{L}_{g1}^{-1}\boldsymbol{B}\right]^{-1}\boldsymbol{B}^{\mathrm{T}}\boldsymbol{L}_{g1}^{-T}\boldsymbol{q}_{d1}\\
&\quad - \frac{1}{\sqrt{2}}\begin{bmatrix} \boldsymbol{I}_m \\ -\boldsymbol{I}_m \end{bmatrix}\left[\boldsymbol{B}^{\mathrm{T}}\boldsymbol{L}_{g2}^{-T}\boldsymbol{L}_{g2}^{-1}\boldsymbol{B}\right]^{-1}\boldsymbol{B}^{\mathrm{T}}\boldsymbol{L}_{g2}^{-T}\boldsymbol{q}_{d2}.
\end{aligned} \tag{20}
$$

Equation (20) gives the optimal control forces to best achieve the desired shape of the entire structure. Since the actuating forces are designed by considering two substructures instead of the entire structure, the computation needed for finding the actuating forces is greatly reduced.

3. Rotational periodic structures

3.1. Modeling and governing equations

A rotational periodic structure is composed of a set of identical substructures evenly distributed along a circle. In other words, a rotational periodic structure with n substructures can be obtained by rotating a substructure by an angle of $\psi = \frac{2\pi}{n}$ around a fixed line for n times. A typical rotational periodic is shown in figure 2, which represents a parabolic dish antenna.

Denoting by $\boldsymbol{w}_k$ the displacement function or function vector of the kth substructure, the control equations and their boundary conditions can be expressed as

$$
\boldsymbol{L}\boldsymbol{w}_k + \boldsymbol{B}\boldsymbol{U}_k = \boldsymbol{0} \qquad \text{in } \Omega, \quad k = 1, 2, \ldots, n \tag{21}
$$

$$
\boldsymbol{\Gamma}\boldsymbol{w}_k = \boldsymbol{0} \qquad \text{on } \partial\Omega, \quad k = 1, 2, \ldots, n \tag{22}
$$

where Ω represents the space occupied by the kth substructure, and $\partial\Omega$ its boundary excluding the common boundary between it and $(k + 1)$th and $(k - 1)$th substructures.

At the interface b_k^- between the $(k - 1)$th and the kth substructures and the interface b_k^+ the kth and the $(k + 1)$th substructures, the continuity conditions of the displacements and generalized forces must be imposed, which are expressed by

$$
\boldsymbol{J}_0\boldsymbol{w}_k|_{b_k^+} = \boldsymbol{J}_0\boldsymbol{w}_{k+1}|_{b_{k+1}^-} \qquad k = 1, 2, \ldots, n \tag{23}
$$

where $\boldsymbol{J}_0$ is a differential operator matrix. It should be noted that $\boldsymbol{w}_{n+1} \equiv \boldsymbol{w}_1$ and $b_{n+1}^- \equiv b_1^-$ for the rotational periodic structure.

If there are l_p rigid or elastic constraints among substructures, the constraining equations can be expressed as follows:

$$\boldsymbol{J}_{pj}\boldsymbol{w}_k|_{s_{pj}} = \overline{\boldsymbol{J}}_{pj}\boldsymbol{w}_{k+p}|_{\overline{s}_{pj}}$$
$$k = 1, 2, \ldots, n; \quad p = 1, 2, \ldots, n-1; \quad j = 1, 2, \ldots, l_p \tag{24}$$

where $\boldsymbol{J}_{pj} (p = 1, 2, \ldots, n-1)$ is a differential operator matrix. Equation (24) gives the constraints between the region s_{pj} (either a point or two- to three-dimensional region) in the kth substructure and the region $\overline{s}_{pj}$ in the $(k+p)$th substructure. The subscript of $\boldsymbol{w}_{k+p}$ should be set to i when it reaches $n+i$.

Due to the continuous conditions in equation (23) and the constraints in equation (24) among substructures, $\boldsymbol{w}_k$ $(k = 1, 2, \ldots, n)$ are coupled with each other. If equations (21)–(24) are used directly to obtain the displacements, the coupled equations of $\boldsymbol{w}_1$ to $\boldsymbol{w}_k$ have to be solved.

3.2. Simplification of the shape control problem

To decouple equations (21)–(24), take the following transformation:

$$\boldsymbol{w} = \{\boldsymbol{w}_1, \boldsymbol{w}_2, \ldots, \boldsymbol{w}_n\}^{\mathrm{T}}$$
$$= [\,\boldsymbol{R}_1 \quad \boldsymbol{R}_2 \quad \cdots \quad \boldsymbol{R}_n\,]\begin{Bmatrix} \boldsymbol{q}_1 \\ \boldsymbol{q}_2 \\ \vdots \\ \boldsymbol{q}_n \end{Bmatrix} = \boldsymbol{R}\boldsymbol{q} \tag{25}$$
$$R_r = \frac{1}{\sqrt{n}}\left[I, \mathrm{e}^{\mathrm{i}r\psi}I, \ldots, \mathrm{e}^{\mathrm{i}r(n-1)\psi}I\right]^{\mathrm{T}}, \qquad r = 1, 2, \ldots, n$$

where $\boldsymbol{q} = (\boldsymbol{q}_1, \boldsymbol{q}_2, \cdots, \boldsymbol{q}_n)^{\mathrm{T}}$ is a new set of generalized displacement functions; $\boldsymbol{I}$ is the identity matrix with the same dimension as w_k. It can be easily proved that the transformation matrix $\boldsymbol{R}$ is a U-matrix, which satisfies

$$\overline{\boldsymbol{R}}^{\mathrm{T}}\boldsymbol{R} = \boldsymbol{I} \tag{26}$$

where the dimension of the identity matrix $\boldsymbol{I}$ is n times that of $\boldsymbol{w}_n$. Taking the same transformation in the actuating force gives

$$\boldsymbol{U} = \{\boldsymbol{U}_1, \boldsymbol{U}_2, \ldots, \boldsymbol{U}_n\}^{\mathbf{T}}$$
$$= [\,\boldsymbol{R}'_1 \quad \boldsymbol{R}'_2 \quad \cdots \quad \boldsymbol{R}'_n\,]\begin{Bmatrix} \boldsymbol{v}_1 \\ \boldsymbol{v}_2 \\ \vdots \\ \boldsymbol{v}_n \end{Bmatrix} = \boldsymbol{R}'\boldsymbol{V} \tag{27}$$
$$R'_r = \frac{1}{\sqrt{n}}\left[I, \mathrm{e}^{\mathrm{i}r\psi}I, \ldots, \mathrm{e}^{\mathrm{i}r(n-1)\psi}I\right]^{\mathrm{T}}, \qquad r = 1, 2, \ldots, n$$

where the dimension of $\boldsymbol{I}$ is the same as those of $\boldsymbol{U}_k$.

Combine the governing equations in equations (21)–(24) into the following forms:

$$\boldsymbol{L}'\boldsymbol{w} + \boldsymbol{B}'\boldsymbol{U} = \boldsymbol{0} \qquad \text{in } \boldsymbol{\Omega}' \tag{28a}$$
$$\boldsymbol{\Gamma}'\boldsymbol{w} = \boldsymbol{0} \qquad \text{on } \partial\boldsymbol{\Omega}' \tag{28b}$$
$$\boldsymbol{J}'_0\boldsymbol{w}|_{b^+} = \boldsymbol{J}'_0\boldsymbol{Y}\boldsymbol{w}|_{b^-} \tag{28c}$$
$$\boldsymbol{J}'_{pj}\boldsymbol{w}|_{s_{pj}} = \overline{\boldsymbol{J}}'_{pj}\boldsymbol{Y}^p\boldsymbol{w}|_{\overline{s}_{pj}}$$
$$p = 1, 2, \ldots, n-1, \quad j = 1, 2, \ldots, l_p \tag{28d}$$

where $\boldsymbol{L}'$, $\boldsymbol{\Gamma}'$, $\boldsymbol{B}'$, $\boldsymbol{J}'_0$ and $\boldsymbol{J}'_{pj}$, $\overline{\boldsymbol{J}}'_{pj}$ $(p = 1, 2, \ldots, n-1)$ are block-diagonal matrices composed of $\boldsymbol{L}$, $\boldsymbol{\Gamma}$, $\boldsymbol{B}$, $\boldsymbol{J}_0$ and $\boldsymbol{J}_{pj}$, $\overline{\boldsymbol{J}}_{pj}$, respectively, $\boldsymbol{\Omega}'$ and $\partial\boldsymbol{\Omega}'$ are the region and boundary of the whole structure and

$$\boldsymbol{Y} = \begin{bmatrix} 0 & \boldsymbol{I} & & & & \\ & 0 & \boldsymbol{I} & & & \\ & & \cdot & \cdot & & \\ & & & \cdot & \cdot & \\ & & & & \cdot & \cdot \\ & & & & 0 & \boldsymbol{I} \\ \boldsymbol{I} & & & & & 0 \end{bmatrix}$$

$$\boldsymbol{Y}^p = \begin{array}{c} \begin{matrix} & & & p+1 & & & \end{matrix} \\ \begin{bmatrix} 0 & \cdot & 0 & \boldsymbol{I} & 0 & \cdot & 0 \\ 0 & \cdot & 0 & 0 & \boldsymbol{I} & \cdot & 0 \\ \cdot & \cdot & \cdot & \cdot & \cdot & \cdot & \cdot \\ 0 & 0 & 0 & \cdot & \cdot & \cdot & \boldsymbol{I} \\ \boldsymbol{I} & 0 & 0 & \cdot & \cdot & \cdot & 0 \\ \cdot & \cdot & \cdot & \cdot & \cdot & \cdot & \cdot \\ 0 & \cdot & \boldsymbol{I} & 0 & 0 & \cdot & 0 \end{bmatrix} \\ \begin{matrix} & & p & & & & \end{matrix} \end{array} . \tag{29}$$

$\boldsymbol{Y}^p$ is a row transformation matrix that satisfies

$$\overline{\boldsymbol{R}}^{\mathrm{T}}\boldsymbol{Y}^p\boldsymbol{R} = \mathrm{diag}(\,\mathrm{e}^{\mathrm{i}p\psi}\boldsymbol{I} \quad \mathrm{e}^{\mathrm{i}2p\psi}\boldsymbol{I} \quad \cdots \quad \mathrm{e}^{\mathrm{i}np\psi}\boldsymbol{I}\,)\,. \tag{30}$$

After substituting equations (25) and (27) into (28), pre-multiplying with $\overline{\boldsymbol{R}}^{\mathrm{T}}$ and employing the property given in equation (26), we have

$$\boldsymbol{L}\boldsymbol{q}_r + \boldsymbol{B}\boldsymbol{v}_r = \boldsymbol{0} \qquad \text{in } \Omega$$
$$\boldsymbol{\Gamma}\boldsymbol{q}_r = \boldsymbol{0} \qquad \text{on } \partial\Omega$$
$$\boldsymbol{J}_0\boldsymbol{q}_r|_{b^+} = \boldsymbol{J}_0\mathrm{e}^{\mathrm{i}r\psi}\boldsymbol{q}_r|_{b^-}$$
$$J_{pj}q_{rj}|_{s_{pj}} = \overline{J}_{pj}\mathrm{e}^{\mathrm{i}pr\psi}q_{rj}|_{\overline{s}_{pj}}$$
$$r = 1, 2, \ldots, n, \quad p = 1, 2, \ldots, n-1, \quad j = 1, 2, \ldots, l_p. \tag{31}$$

Equation (31) is a set of decoupled complex equations in terms of the new generalized displacement functions. Although equation (31) is a complex equation, its solution for $r = s$ is conjugated with that for $r = n - s$. When $r = n$ or $\frac{n}{2}$ (and n is an even number), equation (31) and its solution are real. For the case where $r \neq n, \frac{n}{2}$, we have

$$\boldsymbol{L}\boldsymbol{q}_r^r + \boldsymbol{B}\boldsymbol{v}_r^r = \boldsymbol{0}; \qquad \boldsymbol{L}\boldsymbol{q}_r^i + \boldsymbol{B}\boldsymbol{v}_r^i = \boldsymbol{0} \qquad \text{in } \Omega$$
$$\boldsymbol{B}\boldsymbol{v}_r^r = \boldsymbol{0}; \qquad \boldsymbol{B}\boldsymbol{v}_r^i = \boldsymbol{0} \qquad \text{on } \partial\Omega$$
$$\boldsymbol{J}_0\boldsymbol{q}_r^r|_{b^+} = \boldsymbol{J}_0(\cos r\psi\boldsymbol{q}_r^r - \sin r\psi\boldsymbol{q}_r^i)|_{b^-}$$
$$\boldsymbol{J}_0\boldsymbol{q}_r^i|_{b^+} = \boldsymbol{J}_0(\sin r\psi\boldsymbol{q}_r^r + \cos r\psi\boldsymbol{q}_r^i)|_{b^-}$$
$$\boldsymbol{J}_p\boldsymbol{q}_r^r|_{s_p} = \overline{\boldsymbol{J}}_p(\cos rp\psi\boldsymbol{q}_r^r - \sin rp\psi\boldsymbol{q}_r^i)|_{\overline{s}_p} \tag{32}$$
$$\boldsymbol{J}_p\boldsymbol{q}_r^i|_{s_p} = \overline{\boldsymbol{J}}_p(\sin rp\psi\boldsymbol{q}_r^r + \cos rp\psi\boldsymbol{q}_r^i)|_{\overline{s}_p}$$
$$p = 1, 2, \ldots, n-1 \quad r = 1, 2, \ldots, \frac{n-2}{2} \text{ (even } n\text{)}$$
$$\text{or } \frac{n-1}{2} \text{ (odd } n\text{)}.$$

Hence, it can be concluded that the shape control problem of an entire rotational periodic structure governed by equations (21)–(24) can be simplified to the shape control of its substructures described by equations (31).

Taking the transformation given in equation (25), the desired displacements for the substructures in the new coordinate system are given by

$$\boldsymbol{q}_d = \begin{Bmatrix} \boldsymbol{q}_{d1} \\ \boldsymbol{q}_{d2} \\ \vdots \\ \boldsymbol{q}_{dn} \end{Bmatrix} = \overline{\boldsymbol{R}}^T \boldsymbol{w}_d \tag{33}$$

where $\boldsymbol{w}_d$ is the desired real displacement function vector for the whole structure and $\boldsymbol{q}_{dr} = \boldsymbol{q}^r_{dr} + \mathrm{i}\boldsymbol{q}^i_{dr} (r = 1, 2, \ldots, n)$ is the desired generalized displacements in equation (32). It is easy to verify that $\boldsymbol{q}_{dr}$ is real for $r = n$ and $n/2$ (if n is even). Following the same procedure, the optimal generalized control forces $\boldsymbol{v}_r = \boldsymbol{v}^r_r + \mathrm{i}\boldsymbol{v}^i_r, r = 1, 2, \ldots, n$, can be obtained for the shape control problem of each substructure independently. Then the optimal control forces $\boldsymbol{U} = \{\boldsymbol{U}_1, \boldsymbol{U}_2, \ldots, \boldsymbol{U}_n\}^T$ can be obtained from the transformation of equation (27). In fact, the real and imaginary part of each element $\boldsymbol{U}_r = \boldsymbol{U}^r_r + \mathrm{i}\boldsymbol{U}^i_r$ in the control force vector $\boldsymbol{U}$ can be calculated by

$$\begin{Bmatrix} U^r_r \\ U^i_r \end{Bmatrix} = \begin{bmatrix} \mathrm{I} & 0 \\ \cos r\psi \mathrm{I} & -\sin r\psi \mathrm{I} \\ \vdots & \vdots \\ \cos(n-1)r\psi \mathrm{I} & -\sin(n-1)r\psi \mathrm{I} \\ 0 & \mathrm{I} \\ \sin r\psi \mathrm{I} & \cos r\psi \mathrm{I} \\ \vdots & \vdots \\ \sin(n-1)r\psi \mathrm{I} & \cos(n-1)r\psi \mathrm{I} \end{bmatrix} \begin{Bmatrix} \mathrm{v}^r_r \\ \mathrm{v}^i_r \end{Bmatrix}. \tag{34}$$

Although the generalized control forces $\boldsymbol{v}$ may be complex, the imaginary part of the control forces $\boldsymbol{U}$ obtained from equation (27) will be zero due to the fact that the solution of the rth equation in equations (31) is conjugated with that of the $(n-r)$th equation [19].

When the shape control problem is performed using a discrete system, if each substructure in a rotational periodic structure has m degrees of freedom (DOFs), the shape control problem of the whole structure will have $n \times m$ DOFs. However, when using equations given in equations (31), only two (for even n) or one (for odd n) shape control problems with m DOFs and $\frac{n-2}{2}$ (for even n) or $\frac{n-1}{2}$ (for odd n) shape control problems with $2 \times m$ DOFs are to be handled. Thus, the computational load for shape control of such a structure can be considerably reduced.

3.3. Linear periodic structures

A linear periodic structure is a structure composed of a set of substructures with identical geometric, physical and boundary properties evenly distributed on a straight line or a circular arc and the substructures at both of its ends have their own boundary conditions. The method used to simplify shape control problems of rotational periodic structures can also be employed to simplify that of some kinds of linear periodic structures. To this end, a new rotational periodic structure should be generated by doubly or quadruply extending an original linear periodic structure and then joining its two ends together. Such an extension can only be done when the following two pre-requisites are satisfied.

(1) All its substructures' geometric shapes, physical properties and boundary conditions as well as its constraints with other substructures must be symmetrical so that the newly generated rotational periodic structure is also symmetrical.
(2) At the two ends of the original linear structure, the boundary conditions should conform to the restrictions of symmetrical or anti-symmetrical displacements on the corresponding symmetrical planes of the newly generated rotational periodic structure.

4. Chain structures

4.1. Modeling and governing equations

A chain structure is defined as a structure with two fixed ends constructed with a set of identical substructures aligned like a chain in which there is no common boundary but elastic or rigid constraints without mass between two substructures, and the linking region and style between a substructure and its two neighboring substructures are identical. A typical simple chain structure is a mass–spring system that is assembled by n masses linked with $n+1$ identical springs and fixed at both of its ends. A more complicated example of a chain structure is illustrated in figure 3, in each substructure of which there are three springs and a rigid rod.

Actually, a chain structure is a special kind of linear periodic structure and hence its shape control problem can be treated by the method used in the linear periodic structures. However, due to its special features, the shape control problem of a chain structure can be solved by a simpler methodology given in this section.

If identical actuators with the same actuating forces are configured in each substructure of a chain structure, the shape control of such a structure with n substructures can be expressed by the following equations:

$$\boldsymbol{L}\boldsymbol{w}_k + \boldsymbol{B}\boldsymbol{U}_k = \boldsymbol{0} \qquad \text{in } \Omega, \quad k = 1, 2, \ldots, n \tag{35}$$

$$\boldsymbol{\Gamma}\boldsymbol{w}_k = \boldsymbol{0} \qquad \text{on } \partial\Omega, \quad k = 1, 2, \ldots, n \tag{36}$$

$$\boldsymbol{J}_j \boldsymbol{w}_k|_{s_j} = \overline{\boldsymbol{J}}_j \boldsymbol{w}_{k+1}|_{\overline{s_j}} + \overline{\boldsymbol{J}}_j \boldsymbol{w}_{k-1}|_{\overline{s_j}} \qquad k = 1, 2, \ldots, n, \quad j = 1, 2, \ldots, l \tag{37}$$

where $\boldsymbol{w}_k$ is the displacement function vector of the kth substructure and $\boldsymbol{w}_0 \equiv \boldsymbol{w}_{n+1} = \boldsymbol{0}$. Ω and $\partial\Omega$ are, respectively, the domain and boundary of any substructure. Equation (37) is the equation of l constraints provided by elastic springs and rigid rods.

4.2. Simplification of the shape control problem

It is well known that the displacements of a serial identical mass–spring system can be expressed in the following form:

$$\begin{aligned} \boldsymbol{w}^r &= \{\, w^r_1 \quad w^r_2 \quad \cdots \quad w^r_n \,\}^{\mathrm{T}} \\ &= [\, \sin r\psi \quad \sin 2r\psi \quad \cdots \quad \sin nr\psi \,]^{\mathrm{T}} q_r, \\ &\quad r = 1, 2, \ldots, n \end{aligned} \tag{38}$$

where $\psi = \frac{\pi}{n+1}$ and w^r_k is the displacement of the kth mass.

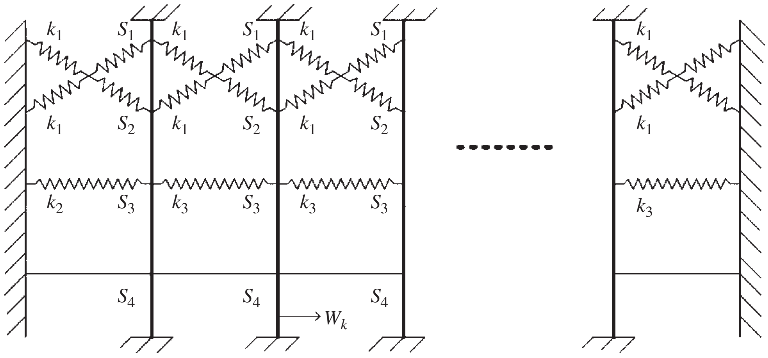

Figure 3. A chain structure.

Inspired by the property given in equation (38), we take the following transformation in the displacement of a general chain structure:

$$w = \begin{Bmatrix} w_1 \\ w_2 \\ \vdots \\ w_n \end{Bmatrix} = \sqrt{\frac{n+1}{2}} \times \begin{bmatrix} \sin\psi I & \cdots & \sin r\psi I & \cdots & \sin n\psi I \\ \sin 2\psi I & \cdots & \sin 2r\psi I & \cdots & \sin 2n\psi I \\ \vdots & \vdots & \vdots & \vdots & \vdots \\ \sin n\psi I & \cdots & \sin rn\psi I & \cdots & \sin nn\psi I \end{bmatrix} \times \begin{Bmatrix} q_1 \\ \vdots \\ q_r \\ \vdots \\ q_n \end{Bmatrix} = Cq \tag{39}$$

where q is the function vector of generalized displacements and the transformation matrix C satisfies

$$C^{\mathrm{T}}C = I \tag{40}$$

$$C^{\mathrm{T}}\left(Y + Y^{n-1}\right)C = \mathrm{diag}(2\cos\psi I, 2\cos 2\psi I, \ldots, 2\cos n\psi I) \tag{41}$$

and Y and Y^{n-1} are given in equation (29).

Similarly, taking the same transformation in the control forces gives

$$U = \begin{Bmatrix} U_1 \\ U_2 \\ \vdots \\ U_n \end{Bmatrix} = \sqrt{\frac{n+1}{2}} \times \begin{bmatrix} \sin\psi I & \cdots & \sin r\psi I & \cdots & \sin n\psi I \\ \sin 2\psi I & \cdots & \sin 2r\psi I & \cdots & \sin 2n\psi I \\ \vdots & \vdots & \vdots & \vdots & \vdots \\ \sin n\psi \mathrm{I} & \cdots & \sin rn\psi I & \cdots & \sin nn\psi I \end{bmatrix} \begin{Bmatrix} v_1 \\ \vdots \\ v_r \\ \vdots \\ v_n \end{Bmatrix} = C'V. \tag{42}$$

Combining the equations of all substructures in equations (35)–(37) gives

$$L'w + B'U = 0 \qquad \text{in } \Omega' \tag{43a}$$

$$\Gamma' w = 0 \qquad \text{on } \partial\Omega' \tag{43b}$$

$$J'_j w|_{s_j} = \overline{J}'_j (Yw|_{\overline{s}_j} + Y^{n-1} w|_{\overline{s_j}}) \qquad j = 1, 2, \ldots, l \tag{43c}$$

where L', Γ', B', J'_j and $\overline{J}'_j$ $(p = 1, 2, \ldots, n-1)$ are the block diagonal matrices assembled by L, Γ, B, J_j and $\overline{J}_j$, respectively, and Ω' and $\partial\Omega'$ represent the domain and boundary of the whole structure. Note that $w_1, w_2, \ldots, w_n$ in equations (43) are coupled with each other.

Substituting equations (39) and (42) into (43), pre-multiplying C^T and noting the features given in equations (40) and (41), the following decoupled equations can be obtained:

$$Lq_r + Bv_r = 0 \qquad \text{in } \Omega \tag{44a}$$

$$\Gamma q_r = 0 \qquad \text{on } \partial\Omega \tag{44b}$$

$$J_j q_r|_{s_j} = \overline{J}_j 2\cos r\psi q_r|_{\overline{s}_j} \qquad r = 1, 2, \ldots, n, \quad j = 1, 2, \ldots, l. \tag{44c}$$

Equations (44) indicate that the shape control problem of a chain structure can be converted to those of its substructures, and thus the computation load can be greatly reduced.

The generalized desired displacements can be obtained from the given target displacement w_d as

$$q_d = C^T w_d. \tag{45}$$

Once the optimal generalized control forces v_r are determined for the given desired shape $q_{\mathrm{d}r}$, the control forces for the entire structure can be calculated by

$$U_r = \{U_{r1}, U_{r2}, \cdots U_{rn}\}^{\mathrm{T}} = [\sin r\psi I, \sin 2r\psi I, \ldots \sin nr\psi I]^{\mathrm{T}} v_r \qquad r = 1, 2, \ldots, n. \tag{46}$$

5. Axisymmetrical structures

5.1. Model and governing equations

A structure is said to be an axisymmetrical structure if its geometrical and physical properties and boundary conditions remain unchanged after being rotated through an arbitrary angle around a straight line. Taking this straight line to be the z-axis in a cylindrical coordinate system, $Or\theta z$, the geometrical and physical properties as well as the boundary conditions of an axisymmetrical structure are independent of θ.

The governing equations and boundary conditions of a three-dimensional continuous axisymmetrical structure can be expressed as

$$
\begin{aligned}
&\boldsymbol{L}_{r,\theta,z}(r,z)[w_r(r,\theta,z),\ w_\theta(r,\theta,z),\ w_z(r,\theta,z)]\\
&\quad + \boldsymbol{B}_{r,\theta,z}(r,z)[U_r(r,\theta,z), U_\theta(r,\theta,z), U_z(r,\theta,z)] = 0\\
&\quad \text{in } \Omega \qquad (47)\\
&\Gamma_{r,\theta,z}(r,z)\left[w_r(r,\theta,z), w_\theta(r,\theta,z), w_z(r,\theta,z)\right] = 0\\
&\quad \text{on } \partial\Omega
\end{aligned}
$$

where Ω represents a three-dimensional domain in the cylindrical coordinate system $Or\theta z$, w_r, w_θ and w_z are the displacements in the directions of r, θ and z, respectively, and $\boldsymbol{L}_{r,\theta,z}$, $\boldsymbol{B}_{r,\theta,z}$ and $\boldsymbol{\Gamma}_{r,\theta,z}$ are the elastic, control and boundary condition operator matrices, respectively, which are independent of θ due to the axisymmetry of the structure.

5.2. Simplification of the shape control problem

The displacements w_r, w_θ and w_z of a three-dimensional axisymmetrical structure can be expanded in the following Fourier series of θ:

$$
\begin{aligned}
w_r(r,\theta,z) &= \sum_{n=0}^{\infty}\left[W_{rn}(r,z)\cos n\theta + W'_{rn}(r,z)\sin n\theta\right]\\
w_\theta(r,\theta,z) &= \sum_{n=0}^{\infty}\left[W'_{\theta n}(r,z)\sin n\theta + W_{\theta n}(r,z)\cos n\theta\right]\\
w_z(r,\theta,z) &= \sum_{n=0}^{\infty}\left[W_{zn}(r,z)\cos n\theta + W'_{zn}(r,z)\sin n\theta\right].
\end{aligned}
\tag{48}
$$

Similarly, the three components of the control force U can also be expanded as

$$
\begin{aligned}
U_r(r,\theta,z) &= \sum_{n=0}^{\infty}\left[U_{rn}(r,z)\cos n\theta + U'_{rn}(r,z)\sin n\theta\right]\\
U_\theta(r,\theta,z) &= \sum_{n=0}^{\infty}\left[U'_{\theta n}(r,z)\sin n\theta + U_{\theta n}(r,z)\cos n\theta\right]\\
U_z(r,\theta,z) &= \sum_{n=0}^{\infty}\left[U_{zn}(r,z)\cos n\theta + U'_{zn}(r,z)\sin n\theta\right].
\end{aligned}
\tag{49}
$$

Substituting equations (48) and (49) into (47) and employing the orthogonality of $\cos n\theta$ and $\sin n\theta$, the following decoupled equations can be obtained for each harmonic component:

$$
\begin{aligned}
&\boldsymbol{L}_{r,\theta,z}(r,z)[W_{rn}\cos n\theta + W'_{rn}\sin n\theta,\ W'_{\theta n}\sin n\theta\\
&\quad +\ W_{\theta n}\cos n\theta,\ W_{zn}\cos n\theta + W'_{zn}\sin n\theta]\\
&\quad + \boldsymbol{B}_{r,\theta,z}(r,z)[U_{rn}\cos n\theta + U'_{rn}\sin n\theta,\ U'_{\theta n}\sin n\theta\\
&\quad +\ U_{\theta n}\cos n\theta,\ U_{zn}\cos n\theta + U'_{zn}\sin n\theta] = 0 \qquad (50)\\
&\quad \text{in } \Omega\\
&\Gamma_{r,\theta,z}(r,z)[W_{rn}\cos n\theta + W'_{rn}\sin n\theta,\ W'_{\theta n}\sin n\theta\\
&\quad +\ W_{\theta n}\sin n\theta,\ W_{zn}\cos n\theta + W'_{zn}\sin n\theta] = 0\\
&\quad \text{on } \partial\boldsymbol{\Omega}.
\end{aligned}
$$

The displacements of an axisymmetrical structure have the following form:

$$
W_n = \begin{bmatrix} W_{rn}(r,z)\cos n\theta \\ W'_{\theta n}(r,z)\sin n\theta \\ W_{zn}(r,z)\cos n\theta \end{bmatrix} + \begin{bmatrix} W'_{rn}(r,z)\sin n\theta \\ W_{\theta n}(r,z)\cos n\theta \\ W'_{zn}(r,z)\sin n\theta \end{bmatrix};\quad n = 0, 1, 2, \ldots. \tag{51}
$$

Clearly, the first term of the displacement in equation (51) is the symmetrical part, and the second term is the anti-symmetrical part. Following the same procedure, the control force can also be separated into symmetrical and anti-symmetrical terms

$$
U_n = \begin{bmatrix} U_{rn}(r,z)\cos n\theta \\ U'_{\theta n}(r,z)\sin n\theta \\ U_{zn}(r,z)\cos n\theta \end{bmatrix} + \begin{bmatrix} U'_{rn}(r,z)\sin n\theta \\ U_{\theta n}(r,z)\cos n\theta \\ U'_{zn}(r,z)\sin n\theta \end{bmatrix};\quad n = 0, 1, 2, \ldots. \tag{52}
$$

Due to the axisymmetry of an axisymmetrical structure with axisymmetrical actuators, it is easy to prove that symmetrical control forces can only actuate symmetrical displacements and anti-symmetrical forces can only actuate anti-symmetrical displacements. Therefore, the following conclusions can be drawn.

(1) The displacements of a three-dimensional axisymmetrical structure can be expressed as the sum of symmetrical and anti-symmetrical displacements, as given in equation (51), and the circumferential components are harmonic waves with order n ($n = 0, 1, 2, \ldots$).

(2) A three-dimensional problem can be solved by converting it to a two-dimensional problem. Consider the symmetrical case in equation (47), i.e.

$$
\boldsymbol{L}_{r,\theta,z}(r,x)\begin{bmatrix} W_{rn}\cos n\theta \\ W'_{\theta n}\sin n\theta \\ W_{zn}\cos n\theta \end{bmatrix} + \boldsymbol{B}_{r,\theta,z}(r,z)\begin{bmatrix} U_{rn}\cos n\theta \\ U'_{\theta n}\sin n\theta \\ U_{zn}\cos n\theta \end{bmatrix} = 0 \tag{53}
$$

$$
\boldsymbol{\Gamma}_{r,\theta,z}(r,z)\begin{bmatrix} W_{rn}\cos n\theta \\ W'_{\theta n}\sin n\theta \\ W_{zn}\cos n\theta \end{bmatrix} = 0. \tag{54}
$$

Since $\boldsymbol{L}_{r,\theta,z}$, $\boldsymbol{\Gamma}_{r,\theta,z}$ and $\boldsymbol{B}_{r,\theta,z}$ are linear operators and independent of θ, the Fourier transformation of equation (53) will include $\cos n\theta$ and $\sin n\theta$ only, and therefore equation (53) is equivalent to the following equations:

$$
\begin{aligned}
&\int_{-\pi}^{\pi}\begin{bmatrix} \cos n\theta & 0 & 0 \\ 0 & \sin n\theta & 0 \\ 0 & 0 & \cos n\theta \end{bmatrix}\left\{ L_{r,\theta,z}(r,z)\begin{bmatrix} W_{rn}\cos n\theta \\ W'_{\theta n}\sin n\theta \\ W_{zn}\cos n\theta \end{bmatrix}\right.\\
&\qquad\left. + B_{r,\theta,z}(r,z)\begin{bmatrix} U_{rn}\cos n\theta \\ U'_{\theta n}\sin n\theta \\ U_{zn}\cos n\theta \end{bmatrix}\right\}\mathrm{d}\theta = 0
\end{aligned}
\tag{55a}
$$

$$
\begin{aligned}
&\int_{-\pi}^{\pi}\begin{bmatrix} \sin n\theta & 0 & 0 \\ 0 & \cos n\theta & 0 \\ 0 & 0 & \sin n\theta \end{bmatrix}\left\{ L_{r,\theta,z}(r,z)\begin{bmatrix} W_{rn}\cos n\theta \\ W'_{\theta n}\sin n\theta \\ W_{zn}\cos n\theta \end{bmatrix}\right.\\
&\qquad\left. + B_{r,\theta,z}(r,z)\begin{bmatrix} U_{rn}\cos n\theta \\ U'_{\theta n}\sin n\theta \\ U_{zn}\cos n\theta \end{bmatrix}\right\}\mathrm{d}\theta = 0.
\end{aligned}
\tag{55b}
$$

It can be proved that equation (55*b*) can be automatically satisfied. In fact,

$$
\begin{aligned}
L_{r,\theta,z}(r,z)\begin{bmatrix} W_{rn}\cos n\theta \\ W'_{\theta n}\sin n\theta \\ W_{zn}\cos n\theta \end{bmatrix} &= \begin{bmatrix} F_1(r,z)\cos n\theta \\ F_2(r,z)\sin n\theta \\ F_3(r,z)\cos n\theta \end{bmatrix}\\
&\quad + \begin{bmatrix} F'_1(r,z)\sin n\theta \\ F'_2(r,z)\cos n\theta \\ F'_3(r,z)\sin n\theta \end{bmatrix}.
\end{aligned}
\tag{55b-1}
$$

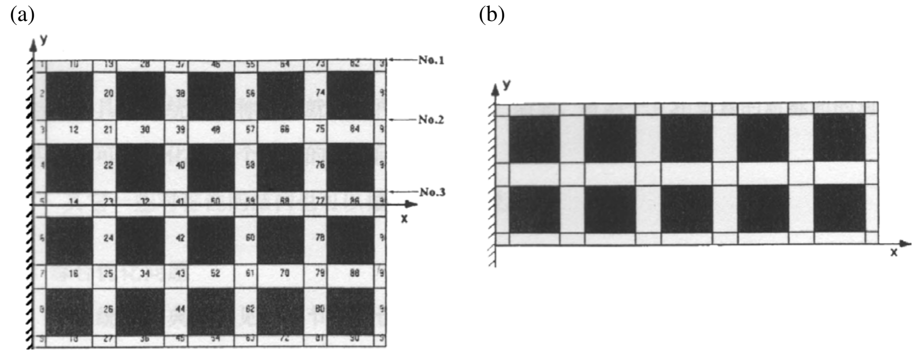

Figure 4. A cantilever symmetrical plate with piezoelectric actuator patches. (a) Original structure with element numbers; (b) its substructure.

Due to the symmetry of an axisymmetrical structure, if we use another cylindrical coordinate system $Or'\theta'z'$, where only the direction of θ' is opposite to that of θ in the original coordinates, and the directions of the other two axes are kept unchanged, we have $L_{r,\theta',z}(r',z') = L_{r,\theta,z}(r,z)$. Thus,

$$
\begin{aligned}
L_{r,\theta',z}(r',z')\begin{bmatrix} W_{rn}\cos n\theta' \\ W'_{\theta n}\sin n\theta' \\ W_{zn}\cos n\theta' \end{bmatrix} &= \begin{bmatrix} F_1(r,z)\cos n\theta' \\ F_2(r,z)\sin n\theta' \\ F_3(r,z)\cos n\theta' \end{bmatrix} + \begin{bmatrix} F'_1(r,z)\sin n\theta' \\ F'_2(r,z)\cos n\theta' \\ F'_3(r,z)\sin n\theta' \end{bmatrix} \\
&= \begin{bmatrix} F_1(r,z)\cos n\theta \\ -F_2(r,z)\sin n\theta \\ F_3(r,z)\cos n\theta \end{bmatrix} + \begin{bmatrix} -F'_1(r,z)\sin n\theta \\ F'_2(r,z)\cos n\theta \\ -F'_3(r,z)\sin n\theta \end{bmatrix}. \qquad (55b\text{-}2)
\end{aligned}
$$

Compared with equation (55b-1), it can be found that the second term on the right-hand side of equation (55b-2) should be zero, that is,

$$
L_{r,\theta,z}(r,z)\begin{bmatrix} W_{rn}\cos n\theta \\ W'_{\theta n}\sin n\theta \\ W_{zn}\cos n\theta \end{bmatrix} = \begin{bmatrix} F_1(r,z)\cos n\theta \\ F_2(r,z)\sin n\theta \\ F_3(r,z)\cos n\theta \end{bmatrix}.
$$

Similarly, $B_{r,\theta,z}(r,z)\begin{bmatrix} U_{rn}\cos n\theta \\ U'_{\theta n}\sin n\theta \\ U_{zn}\cos n\theta \end{bmatrix}$ has the same property, and hence equation (55b) must be satisfied.

Rewrite equation (55a) in the following form:

$$
\begin{aligned}
&\left(\int_{-\pi}^{\pi}\begin{bmatrix} \cos n\theta & 0 & 0 \\ 0 & \sin n\theta & 0 \\ 0 & 0 & \cos n\theta \end{bmatrix} \times L_{r,\theta,z}(r,x)\begin{bmatrix} \cos n\theta & 0 & 0 \\ 0 & \sin n\theta & 0 \\ 0 & 0 & \cos n\theta \end{bmatrix}\mathrm{d}\theta\right)\begin{bmatrix} W_{rn} \\ W'_{\theta n} \\ W_{zn} \end{bmatrix} \\
&+\left(\int_{-\pi}^{\pi}\begin{bmatrix} \cos n\theta & 0 & 0 \\ 0 & \sin n\theta & 0 \\ 0 & 0 & \cos n\theta \end{bmatrix} \times \boldsymbol{B}_{r,\theta,z}(r,x)\begin{bmatrix} \cos n\theta & 0 & 0 \\ 0 & \sin n\theta & 0 \\ 0 & 0 & \cos n\theta \end{bmatrix}\mathrm{d}\theta\right) \\
&\times \begin{bmatrix} U_{rn} \\ U'_{\theta n} \\ U_{zn} \end{bmatrix} = 0. \qquad (56a)
\end{aligned}
$$

Similarly, rearrange equation (54) as

$$
\begin{aligned}
&\left(\int_{-\pi}^{\pi}\begin{bmatrix} \cos n\theta & 0 & 0 \\ 0 & \sin n\theta & 0 \\ 0 & 0 & \cos n\theta \end{bmatrix} \times \Gamma_{r,\theta,z}(r,x)\begin{bmatrix} \cos n\theta & 0 & 0 \\ 0 & \sin n\theta & 0 \\ 0 & 0 & \cos n\theta \end{bmatrix}\mathrm{d}\theta\right) \\
&\times \begin{bmatrix} W_{rn} \\ W'_{\theta n} \\ W_{zn} \end{bmatrix} = 0. \qquad (56b)
\end{aligned}
$$

From equation (56), the following equations in terms of W_{rn}, $W'_{\theta n}$, W_{zn} and parameter n can be obtained:

$$
\begin{aligned}
&\boldsymbol{L}_{r,z}(r,x,n)\begin{bmatrix} W_{rn} \\ W'_{\theta n} \\ W_{zn} \end{bmatrix} + \boldsymbol{B}_{r,z}(r,z,n)\begin{bmatrix} U_{rn} \\ U'_{\theta n} \\ U_{zn} \end{bmatrix} = 0 \qquad \text{in } \boldsymbol{\Omega} \\
&\boldsymbol{\Gamma}_{r,z}(r,z,n)\begin{bmatrix} W_{rn} \\ W'_{\theta n} \\ W_{zn} \end{bmatrix} = 0 \qquad \text{on } \partial\boldsymbol{\Omega} \quad n = 1, 2, \ldots. \qquad (57)
\end{aligned}
$$

Equations (57) show that the shape control problem of a three-dimensional axisymmetrical structure in equation (47) can be converted to shape control problems of an infinite number of two-dimensional structures described in equations (57). In engineering practice, only a limited number of the shape control problems are required to solve that of a whole three-dimensional axisymmetrical structure approximately.

6. Illustrative examples

Consider a cantilever rectangular plate bonded with 20 piezoelectric actuator patches, as shown in figure 4. The whole structure and its boundary conditions are symmetrical about the x axis. The length, width and thickness of the host plate are 150, 120 and 2 mm, respectively. The Young's modulus and Poisson's ratio of the host plate are 70 GPa and 0.3, respectively. The dimensions of each actuator patch are 20 mm × 20 mm × 0.25 mm. The distance between any two adjacent actuators is 10 mm and the gap between the actuator patches to the edge is 5 mm. The Young's modulus, Poisson's ratio and piezoelectric stress constant of the 0.5 mm thick piezoelectric actuators are 50 GPa, 0.3 and $e_{31} = e_{32} = 10$ N V m^{-1}, respectively.

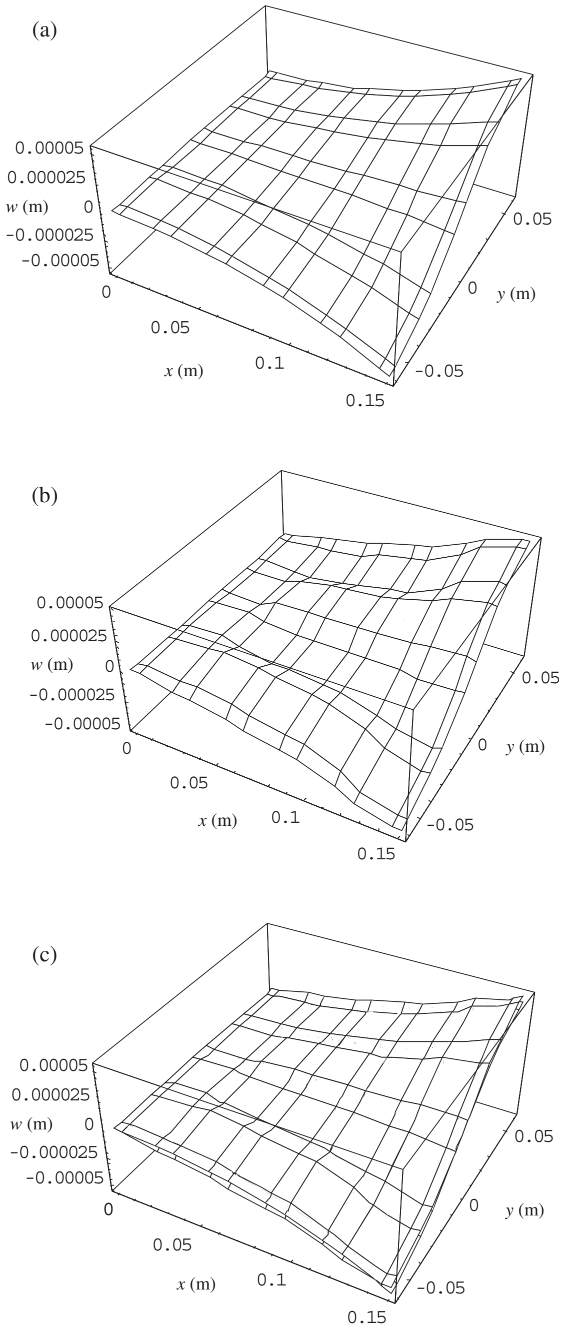

Figure 5. Comparison between the actuated and desired shapes ($A = 0.0001$, $B = 0.0$). (a) Desired shape (anti-symmetrical); (b) actuated shape; (c) actuated and desired shapes.

The desired shape of the composite plate is described by its transverse displacements given by

$$w_d(x, y) = A * (\cosh(x/2a) - 1) * \sin(y * \pi/2b) + B * \left(\frac{x}{2a}\right)^2 * \left[\frac{1}{2}\left(\frac{y}{b}\right)^2 + C\right] \quad (58)$$

where a and b are the half length and half width of the host plate, respectively; A, B and C are parameters used to adjust the desired shape.

Clearly, the desired shape includes an anti-symmetrical part described by

$$w_{\mathrm{da}}(x, y) = A * (\cosh(x/2a) - 1) * \sin(y * \pi/2b),$$

and a symmetrical part described by

$$w_{\mathrm{ds}}(x, y) = B * \left(\frac{x}{2a}\right)^2 * \left[\frac{1}{2}\left(\frac{y}{b}\right)^2 + C\right].$$

To perform the shape control of the plate, the finite element method is employed to discretize the governing equations. An eight-node adhesive element [18] is employed, which combines a pair of collocated four-node quadrilateral elements for the upper and lower piezoelectric plates and a sandwiched pseudo-adhesive layer element. The whole structure is meshed into 99 rectangular elements with 120 nodes. The total number of DOFs is 360 and the number of control voltages is 20.

Since the whole structure is symmetrical about the x axis, according to the simplification method given in section 2, its shape control can be converted to shape control of its substructures. Figure 4(b) shows its substructure which contains 55 plate elements with only 60 nodes plus 12 nodes on the symmetrical axis. Taking the boundary conditions at the fixed end and the constraining equations on the symmetrical axis into account, the total number of DOFs of each substructure is 192 with ten control voltages.

Following the procedure given in section 2.2, the optimal control voltages for the ten actuators in the substructures can be obtained. Firstly, take the anti-symmetrical shape as the desired shape. In this case, the parameters A, B and C in equation (58) are taken as 0.0001, 0.0 and 0.2, respectively. The optimal control voltages for the desired shape are 1780.38, 3324.19, −3324.19, −1780.38, 4457.35, −2811.2, 2811.2, −4457.35, 2911.4, −2667.83, 2667.83, −2911.4, 3868.32, −1750.31, 1750.31, −3868.32, −1683.15, −2779.12, 2779.12 and 1683.15 V, respectively. The actuated shape and the desired one are shown in figures 5(a) and (b). The closeness of the actuated shape to the desired one can be measured by the square error between them. Applying the optimal control voltages to the actuators, the square error between the actuated shape of the whole structure and the desired one is 1.4×10^{-9} m^2.

Secondly, find the optimal control voltage for the symmetrical desired shape, i.e., the parameters A, B and C in equation (58) are taken as 0.0, 0.0001 and 0.2 respectively. The control voltages obtained from equation (20) are 535.171, −20.2231, −20.2231, 535.171, 461.402, −393.121, −393.121, 461.402, 761.591, 1064.71, 1064.71, 761.591, −722.039, −1213.13, −1213.13, −722.039, 1194.72, 4636.4, 4636.4 and 1194.72 V, respectively, which are also symmetrical about the x axis. The actuated shape by the optimal control voltages is given in figure 6(b) and the square error in this case is only 6.0×10^{-10} m^2. Figure 6(c) shows that the actuated shape is very close to the desired one.

Finally, since the controlled plate is a linear system, the final optimal control voltages can be obtained from the superposition of the control voltages of the anti-symmetrical and symmetrical cases. In this case, the optimal control voltages for all actuators are 2315.55, 3303.97, −3344.42, −1245.21, 4918.75, −3204.32, 2418.08, −3995.95, 3673., −1603.12, 3732.55, −2149.81, 3146.28, −2963.44, 537.172, −4590.36, −488.431, 1857.28, 7415.51 and 2877.88 V, respectively. The desired shape and the actuated shape are

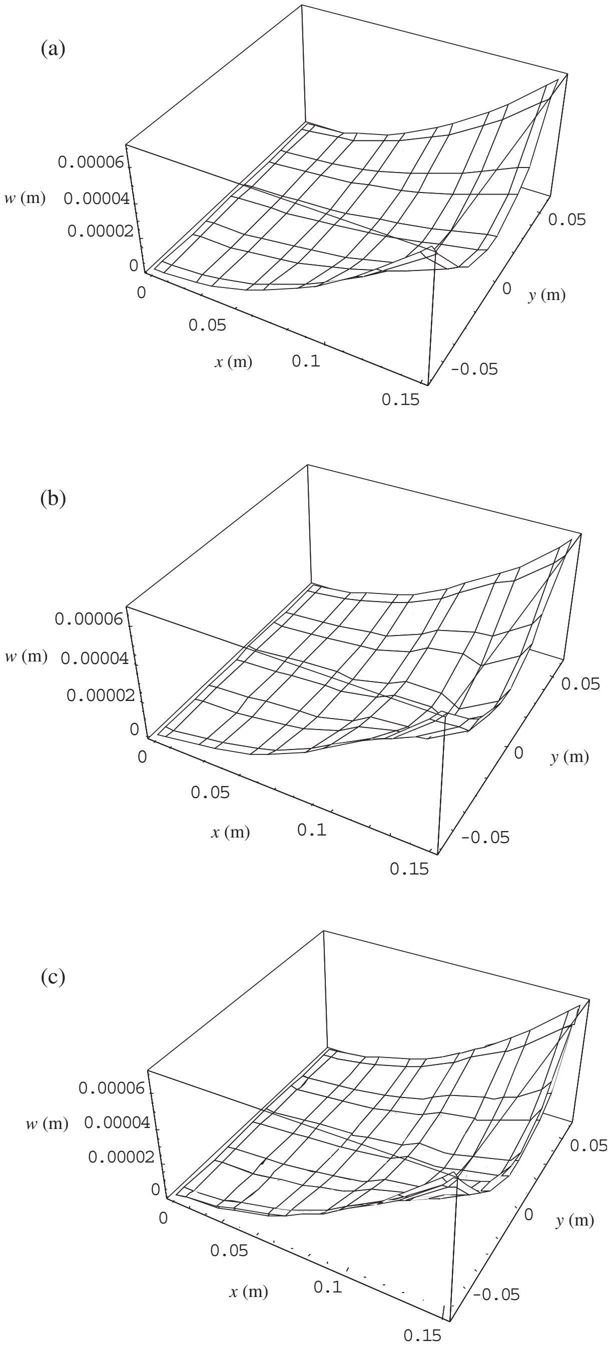

Figure 6. Comparison between the actuated and desired shapes ($A = 0.0$, $B = 0.0001$). (a) Desired shape (symmetrical); (b) actuated shape; (c) actuated and desired shapes.

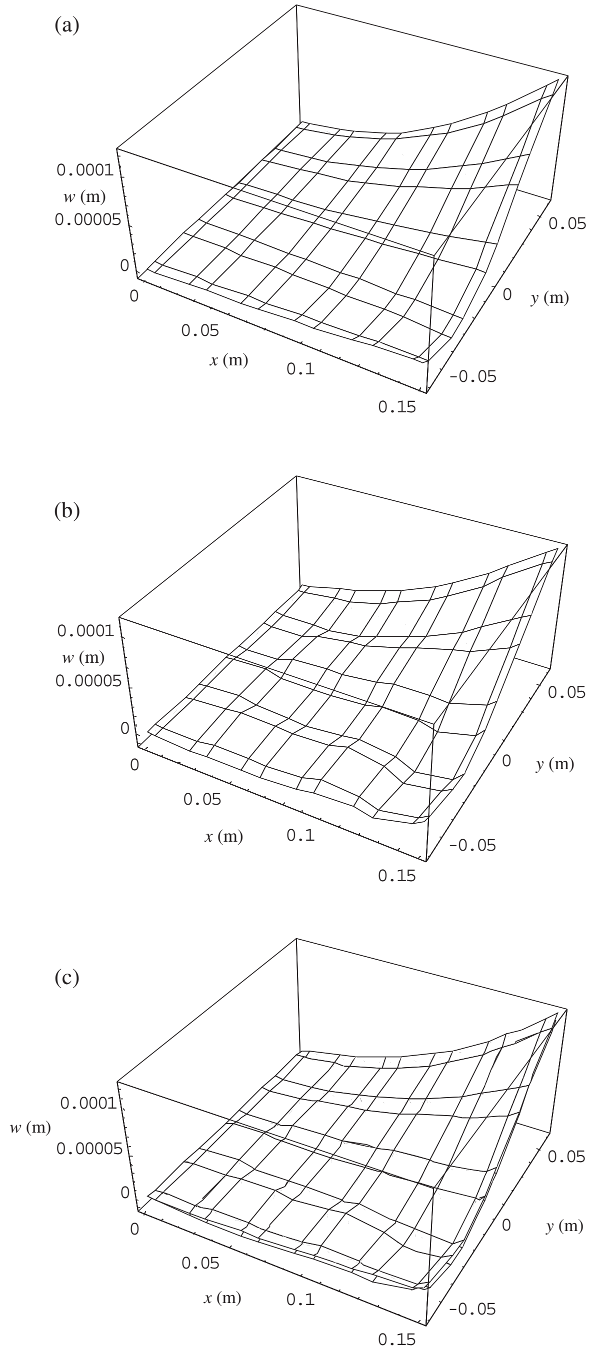

Figure 7. Comparison between the actuated and desired shapes ($A = 0.0001$, $B = 0.0001$). (a) Desired shape (combination of anti-symmetrical and symmetrical shapes); (b) actuated shape; (c) actuated and desired shapes.

shown in figures 7(a) and (b), respectively. In this case, the square error is only 2.0×10^{-9} m^2, which indicates a close match is achieved, as shown in figure 7(c).

As shown in this example, if a desired shape is asymmetrical and can be divided into a symmetrical and an anti-symmetrical one, the simplification methods can be employed in shape control of the linear symmetrical structure. In this case, the optimal control forces (voltages) and the actuated shapes can be obtained by means of the superposition method.

7. Conclusions

In this paper, shape control of some repetitive structures such as symmetrical, rotational periodic, linear periodic, chain and axisymmetrical structures is investigated. Based on their governing equations derived from a continuous model, simplification methods for shape control of these structures are presented by taking advantage of their special features. Employing these simplification methods, the shape control problems of the entire structure with n substructures can be generally converted to n shape control problems of a single substructure, and hence the computation cost can be greatly reduced.

Acknowledgments

The authors are grateful for the support of the National Natural Foundation of China (grant No 60034010) and the Australian Research Council via a Discovery-Projects grant (grant No DP0210716). The fourth author acknowledges the support from Beijing Institute of Spacecraft System Engineering, Chinese Academy of Space Technology.

References

[1] Haftka R T and Adelman H M 1985 An analytical investigation of shape control of large space structures by applied temperatures *AIAA J.* **23** 450–7
[2] Truchi C 1990 Adaptive optics—shape control of an adaptive mirror *Lecture Notes in Control and Information Sciences* vol 147, pp 28–45
[3] Balas M J 1985 Optimal quasi-static shape control for large aerospace antennae *J. Opt. Theory Appl.* **46** 153–70
[4] Austin F, Rossi M J, Vannostrand W, Knowles G and Jameson A 1994 Static shape control for adaptive wings *AIAA J.* **32** 1895–901
[5] Agrawal S K, Tong D Q and Nagaraja K 1994 Modeling and shape control of piezoelectric actuator embedded elastic plates *J. Intell. Mater. Syst. Struct.* **5** 514–21
[6] Ghosh K G and Batra R C 1995 Shape control of plates using piezoceramic elements *AIAA J.* **33** 1354–7
[7] Bruch J C, Sloss J M, Adali S and Sadek I S 2000 Optimal piezo-actuator locations/lengths and applied voltage for shape control of beams *Smart Mater. Struct.* **9** 205–11
[8] Koconis D B, Kollar L P and Springer G S 1994 Shape control of composite plates and shells with embedded actuators. 2. Desired shape specified *J. Compos. Mater.* **28** 459–82
[9] Chee C Y K, Tong L Y and Steven G P 2002 Static shape control of composite plates using a slope–displacement-based algorithm *AIAA J.* **40** 1611–8
[10] Irschik H 2002 A review on static and dynamic shape control of structures by piezoelectric actuation *Eng. Struct.* **24** 5–11
[11] Chee C Y K, Tong L Y and Steven G P 1998 A review on the modelling of piezoelectric sensors and actuators incorporated in intelligent structures *J. Intell. Mater. Syst. Struct.* **9** 3–19
[12] Evensen D A 1976 Vibration analysis of multi-symmetric structures *AIAA J.* **14** 446–53
[13] Thomas D L 1979 Dynamics of rotational periodic structures *Int. J. Numer. Methods Eng.* **14** 81–102
[14] Cai C and Wu F 1983 On the vibration of rotational periodic structures *Acta Scientiarum Naturalium Universitatis Sunyatseni* **22** 109
[15] Cai C, Cheung Y and Chan H 1990 Uncoupling of dynamic equations for periodic structures *J. Sound Vib.* **139** 253–63
[16] Chan H, Cai C and Cheung Y 1998 *Exact Analysis of Structures with Periodicity Using U-Transformation* (Singapore: World Scientific)
[17] Wang D J and Wang C C 2000 Natural vibration of repetitive structures *Chin. J. Mech.* **16** 85–95
[18] Sun D C and Tong L Y 2004 Adhesive element modeling and weighted static shape control of composite plates with piezoelectric actuator patches *Int. J. Numer. Methods Eng.* **60** 1911–32
[19] Wang D J, Zhou C Y and Rong J 2003 Free and forced vibration of repetitive structures *Int. J. Solid Struct.* **40** 5477–94